Environment, Resource and Ecology Journal (2022)
Clausius Scientific Press, Canada

DOI: 10.23977/erej.2022.060408
ISSN 2616-3756 Vol. 6 Num. 4

Analysis of the Water Vapor, Instability Conditions and Dynamics Characteristics of an Extreme Rainstorm Event in Liaoning Province

Ping Li[1], Yu Chen[2,*], Zhongyan Lu[1], Shuo Liu[1], Dan Niu[3]

[1]Liaoning Provincial Meteorological Observatory, Shenyang, China
[2]Liaoning Meteorological Disaster Monitoring and Early Warning Centre, Shenyang, China
[3]Liaoning Province Meteorological Service Center, Shenyang, China
Shenya_lip@163.com

Keywords: Jianghuai Cyclone, extreme rainstorm, Generalized potential temperature

Abstract: This paper presents a diagnostic analysis of the dynamic, thermal, and water vapor characteristics of a regional extreme rainstorm in Liaoning Province on September 19, 2021, using automatic station observations and ERA5 reanalysis data, and concludes that the storm occurred under favorable circulation conditions. The storm had two water vapor belts, which converged in western Liaoning. The front was convectively unstable and symmetrically unstable before the end of the precipitation, and the convective instability weakened as the precipitation intensified. With the front moving rapidly to the northern coast of the Bohai Sea. The frontal center moves northward rapidly and extends down to near 950 hPa and the warm tongue of the high altitude extends down to the south of the frontal surface strengthens, the warm and humid airflow and low altitude rapids occur explosively, causing strong airflow to strengthen the tilted rise and enhance the symmetric instability, which makes the precipitation enhance.

1. Introduction

Liaoning is located in the southern part of northeast China, and heavy rainfall occurs every year, but 90% of them occur from June to August, and it is relatively rare for heavy rainfall to occur in autumn. With the progress of economic construction, the damage caused by heavy rainfall has become more and more significant. Therefore, research on the occurrence mechanism of heavy rainfall and the theory and method of forecasting has been the focus of research[1-6] The basic conditions for the occurrence of persistent heavy rainstorms in China are (1) two weather-scale systems providing systematic upward motion in the intersection region, (2) a constant supply of water vapor, and (3) a potential unstable stratification as an important condition for the occurrence of persistent heavy rainstorms. The inflow of warm and humid air at low altitude is very favorable for the establishment of the geopotential unstable stratification[7].

In recent years, there have been many studies on the main influencing systems, triggering mechanisms and characteristics of ground meteorological elements for heavy rainfall in Liaoning. The main influencing systems of heavy rainfall in Liaoning are the 200 hPa high altitude rapid, the

500 hPa high altitude trough, and the 850 hPa cyclone, shear line and saddle field shear [8]; the low altitude rapid provides the necessary water vapor conditions for heavy rainfall in Liaoning [9]. In the context of favorable large-scale circulation, mesoscale convective systems generated along the shear lines are the main influential systems causing heavy precipitation [10].

2021 September 19-21 (Beijing time, the same below) Liaoning Province, an extreme rainstorm process, the province's average rainfall and maximum rainfall exceeded the historical extreme value of September since 1951. Heavy rainfall and high winds affected the largest range since 2010 in September. Jinzhou and Huludao cities are the first level of heavy rainfall disaster, which is the most serious level. In this paper, we use the automatic station observation data and Eurocenter reanalysis data to make a comprehensive analysis of this extreme rainstorm in Liaoning Province in terms of precipitation characteristics, large-scale environment, water vapor, and dynamics, especially using physical quantities,in order to discover its dynamics and thermodynamic characteristics, promote the understanding of this extreme precipitation event, and provide reference for the analysis and forecast of such extreme weather in the future.

2. Data and Methodology

Observation data: hour-by-hour observation data from 1605 automatic weather stations in Liaoning area from the National Meteorological Information Center.

ERA5 reanalysis data: horizontal resolution of 0.25 °×0.25 °, temporal resolution of 1 hour, and 37 layers from 1000 hPa to 1 hPa in vertical direction, which can be used to analyze therapid evolution process of small and medium scale systems.

3. Results and discussion

3.1 Precipitation profile

Figure. 1 is precipitation profile from 12:00 a.m. on September 19 to 12:00 p.m. on September 21, 2021.Affected by the JAC cyclone, Liaoning Province on September 19-21, 2021, there is the largest impact since 2010 in September, the strongest stormy weather. The average and maximum rainfall in the province exceeded the historical extreme value in September since 1951. Heavy rainfall of 100 mm or more occurred in most areas in western and southern Liaoning (Figure 1a). There were 442 meteorological stations in the province with 100 to 250 mm heavy rainfall, 614 meteorological stations with 50 to 100 mm heavy rainfall, and the number of stations with heavy rainfall accounted for 64% of the province. The average rainfall in the province during this process was 74.8 mm, reaching 1.25 times the total rainfall in September, of which the average rainfall in Jinzhou and Huludao areas were 138 mm and 141.8 mm, reaching the level of heavy rainfall (table omitted); the maximum rainfall in Xudabao Town, Xingcheng City, Huludao (40.42 ℃N, 120.57 ℃E) was 341.5 mm. The hourly precipitation time series map shows that the strong precipitation at this station started at 00:00 on the 20th and reached a peak of 74.7 mm at 05:00 on the 20th, after which the precipitation weakened rapidly (Figure 1b).

Hour-by-hour analysis of heavy precipitation stations (Figure.1c) shows that the period of short-time heavy precipitation was from 18:00 on the 19th to 10:00 on the 20th, with 25 stations greater than or equal to 20 mm-h-1 and 5 stations greater than or equal to 50 mm-h-1 at 05:00 on the 20th. At 06:00 on the 21st, there were 62 stations in Liaoning Province with short-time heavy precipitation (≥20 $mm \cdot h^{-1}$) and 10 stations with extreme short-time heavy precipitation (≥50 $mm\ h^{-1}$). Most of the short-time heavy precipitation during this rainstorm occurred in the coastal areas of Huludao, Jinzhou, Dalian and Dandong areas (Figure 1d).

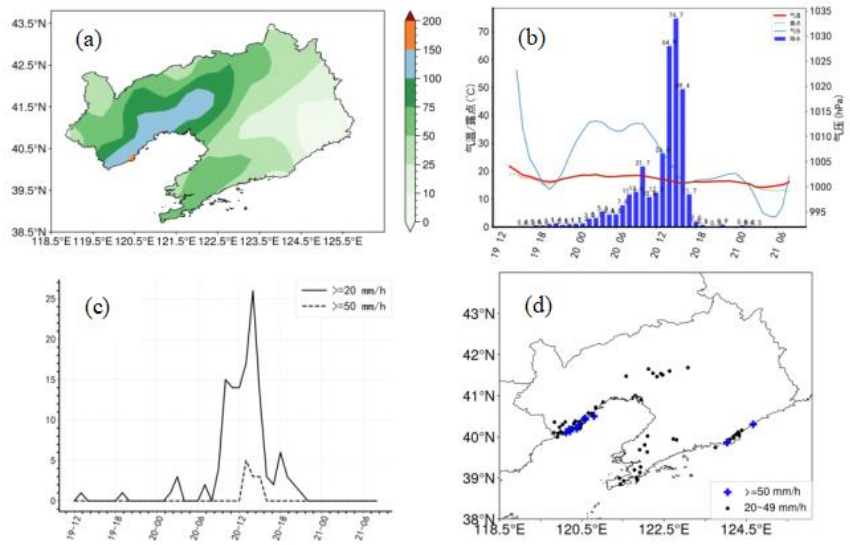

Figure 1: Precipitation profile from 12:00 a.m. on September 19 to 12:00 p.m. on September 21, 2021(a) Accumulated precipitation in Liaoning Province (unit: mm) (b) Time-series of precipitation, pressure, dewpoint, and barometric pressure in Xingcheng, Huludao City (c) Time-series of precipitation stations in Liaoning Province with short-term intense precipitation ≥20 mm•h^{-1} and ≥50 mm•h^{-1}, (d) Distribution map of short-term intense precipitation (blue + indicates precipitation intensity greater than or equal to 50 mm•h^{-1},, black solid dots indicate precipitation intensity between 20 and 49 mm•h^{-1})

3.2 Weather circulation situation

Figure 2 shows weather circulation situation. On the 200 hPa isobar (Figure 2a), the top of the high-pressure ridge was located to the east of Inner Mongolia at 20:00 on the 19th, with a large north-south low-pressure trough to the west and a low trough located at about 109 ℃. Under the influence of the high-pressure ridge, there was an anticyclonic circulation in Liaoning with southwesterly to westerly winds, and it was located to the south of the high rapid area (wind speed greater than or equal to 30 m s^{-1}). On the 500 hPa isobaric surface (Figure 2b), the 500 hPa southwesterly jet (wind speed greater than or equal to 24 m s^{-1}) from eastern Yunnan to northern Bohai Sea at 20:00 on the 19th. On the 850 hPa isobaric surface (Figure 2c), the southeast wind with east wind shear from southern Hebei to the northern Bohai Sea. The maximum southeasterly wind speed near Huludao was 12 m s^{-1}. Strong southeasterly airflow existed on the 925 hPa isobaric surface from the East China Sea to the northern Bohai Sea at 20:00 on the 19th (Figure 2d) due to the influence of the periphery of the subsalt. Low-altitude rapids transport water vapor to the northern Bohai Sea and are blocked by mountains, which pile up and converge and lift on the windward slope in front of the mountains (Huludao coast), promoting the development of precipitation systems. As seen from the ground weather map, the JAC cyclone is located at (26 ℃~36 ℃, 112 ℃~120 ℃) with a central pressure of 1006 hPa, and the Huludao area is located on its northeast side, where there is an obvious convergence of easterly airflow and southeasterly airflow from the East China Sea, providing power and water vapor convergence conditions for the rainstorm (Figure 2e).

To sum up, the deep ridge front in the upper level provides the power conditions for high altitude dispersion; the mid-level high trough guides the low-level JAC cyclone northward, and the low-level and super-low-level rapids and shear lines provide water vapor and power conditions. The

favorable high- and low-altitude configurations caused extreme rainstorms in the Huludao and Jinzhou areas.

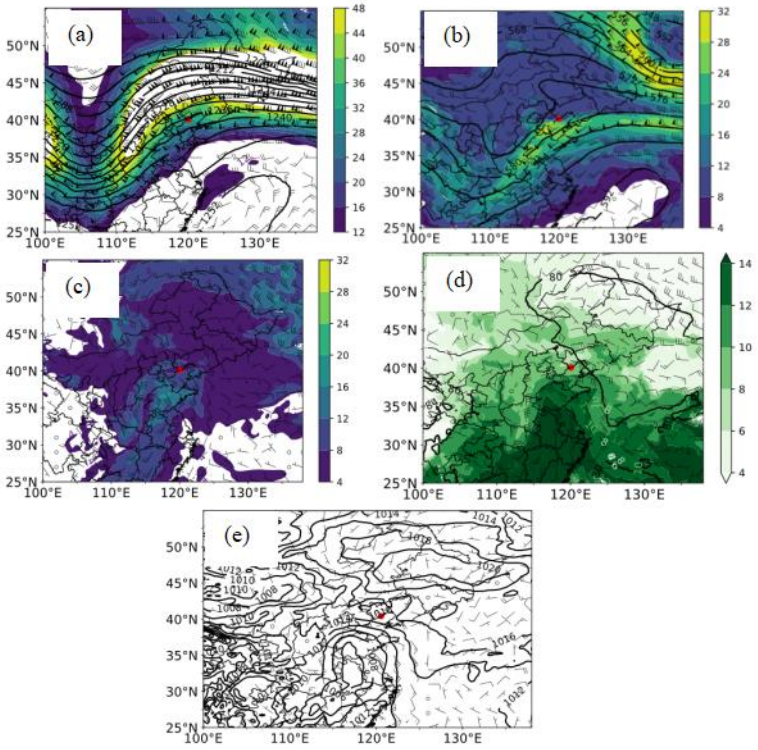

Figure 2: (a) 200 hPa geopotential height (isoline,unit: dgpm) and wind speed (shaded,unit: m•s−1) and wind vector (wind barb, unit:m·s−1) (b) 500 hPa geopotential height (isoline;units:dgpm) and wind speed (shaded,units: m·s−1)1), (c) 850 hPa geopotential height (isoline,units:dgpm) and wind speed (shaded,units:m•s−1) and wind vector (wind barb,unit:m·s−1)1), (d) 925 hPa geopotential height (isoline;unit: dgpm) and specific humidity (shaded,unit: g•kg-1) and wind vector (wind barb,unit:m·s−1)), (e) sea level pressure field (isoline,units:hPa) and wind vector(wind barb,unit: m·s−1)) at 20:00 on September 19, 2021 (Beijing time, same below) . The red dot represents the location of the maximum precipitation site, Xu Dabao Town, Xingcheng City, Huludao.

3.3 Dynamic conditions

From 00:00 on the 20th to 12:00 on the 20th (Figure 3), the cyclonic circulation over Xingcheng City was from 950 to 350 hPa, and the airflow below 900 hPa near the ground was converging in the whole layer. 20:00 on the 20th, the airflow below 900 hPa converged and the vertical motion gradually strengthened, and the area from the ground to 150 hPa was the area of upward motion, and the strong upward center appeared at 850 hPa ~ 550 hPa at 12:00 on the 20th. 550 hPa; at 12:00 on the 21st, due to the sinking and dragging effect of precipitation particles, the sinking motion was dominated by 700 hPa overhead.

At 11:00 on the 20th 200 hPa ~ 500 hPa to the west of Huludao dispersion, high altitude rapids strong (Figure 4a). 500 hPa (Figure 4b) is the airflow wind speed convergence area. At 850 hPa (Fig. 4c), the center of the vortex can be clearly seen as a mesoscale vortex located in the western part of the Bohai Sea, which is very deep. The Huludao area is located in the shear convergence zone of the easterly and southeasterly winds at the top of the vortex. 925 hPa (Fig. 4d) shows the cyclonic circulation in the Huludao area with wind speeds greater than 20 m-s-1, which meets the

boundary layer rapidity criteria. Meanwhile, the southern part of Xingcheng, Suizhong, and Dalian areas are located in the coastal nature and are all higher terrain areas to the north. When encountering topographic obstruction, wind speed convergence is formed in front of the west side of the mountain.

Huludao Xingcheng city area is located in the northern coast of the Bohai Sea, backed by mountainous areas, elevation greater than 500m, at 05:00 on the 20th (Figure 5a) near the ground northeast airflow and easterly airflow into the trumpet terrain, guided by the mesoscale vortex (center located at 34.75 °N), airflow in the north and east side of Mt. climbing, terrain blocking forced to produce convergence upward movement. 11:00 on the 20th (Figure 5b) JAC cyclone slowly north lifting, guiding the strengthening of the easterly airflow, offshore winds climbing at the bottom, and the strengthening easterly winds climbing from the east side of the coastline, making a large amount of water vapor and kinetic energy accumulate in front of the mountains, stimulating and strengthening the development of convection, prompting a significant increase in precipitation.

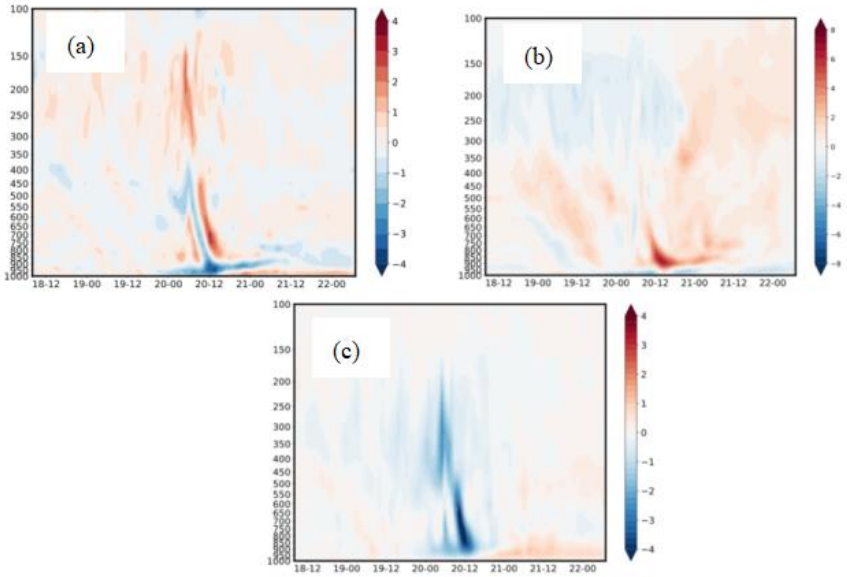

Figure 3: Height-time evolution of (a) divergence (unit: 10−4 s−1), (b) vorticity(unit: 10−4 s−1) and (c) vertical velocity(unit: hPa•s−1), in Xingcheng(40.42°N, 120.57°E) from 18:00 20 September to 08:00 September 22th, 2021

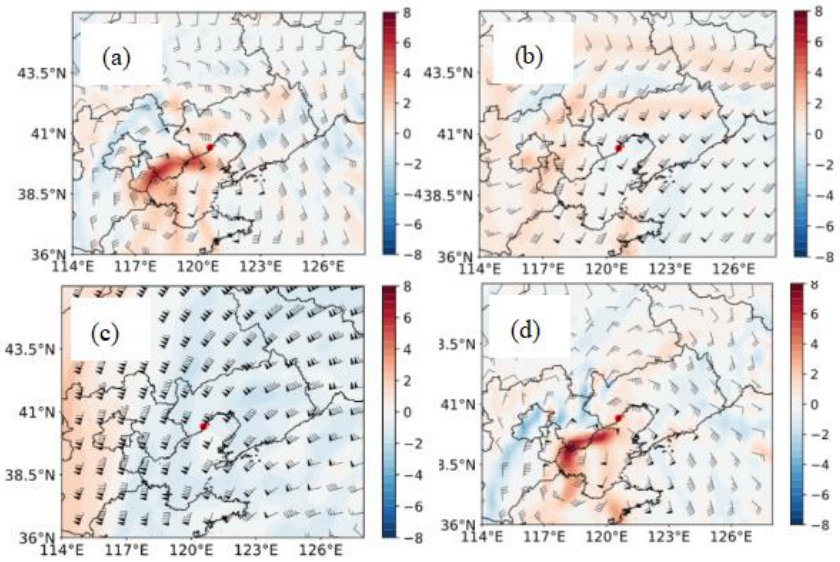

Figure 4: Horizontal distribution of wind vectors (wind barbs,unit: m s-1) and vorticity(shaded,units: 10−4 s−1) at 11:00 on September 20 2021 (a) 200 hPa, (b) 500 hPa, (c) 700 hPa, (d) 925 hPa ,red dots represent Xingcheng location.

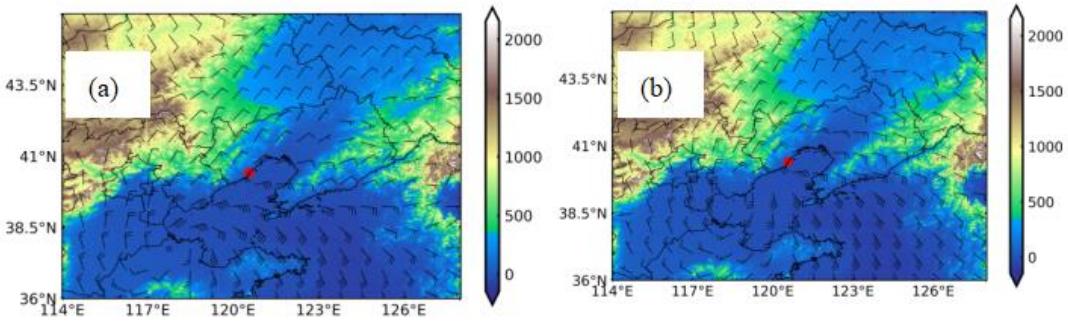

Figure 5: Wind vectors (wind barbs, unit: m•s−1) and vorticity (shaded,units: 10−4 s−1) at 10 meter ground (a)05:00 (b) 11:00 on September 20 2021, red dots represent red dots represent Xingcheng location.

3.4 Water vapor conditions

Abundant water vapor is a necessary condition for the formation of heavy rainfall, and the source of water vapor can be studied by using the whole-atmosphere precipitable water analysis [11]The ERA5 reanalysis data were used to calculate the whole atmospheric precipitable water (PW), and it was found that the high value area of PW greater than 40 mm at 05:00 on the 20th was in a north-south band, extending from southern China to southern and western Liaoning (Figure 6a); the precipitable water was greater than 40 mm in the whole Liaoning region at 02:00 on the 20th, and greater than 45 mm in the western and southern coastal areas (Figure 6b).

There are two sources of water vapor for this precipitation process, a southwest rapid (wind speed >12 m s^{-1}) and also a strong convergence center of water vapor flux (less than -8 × 10^{-4} kg m^{-2} s^{-1}). The rapids transport water vapor to the Liaoning region through the high value

precipitable area. Another relatively weak water vapor conveyor belt (weaker water vapor convergence center and high precipitable area) is transported northward from eastern Jiangsu to Dalian via the Yellow Sea. These two water vapor conveyor belts converge in western Liaoning and form water vapor flux convergence centers near the Huludao (blue and red dotted areas in the figure) and Jinzhou areas to supply water vapor for the storm (Figure 6c, d).

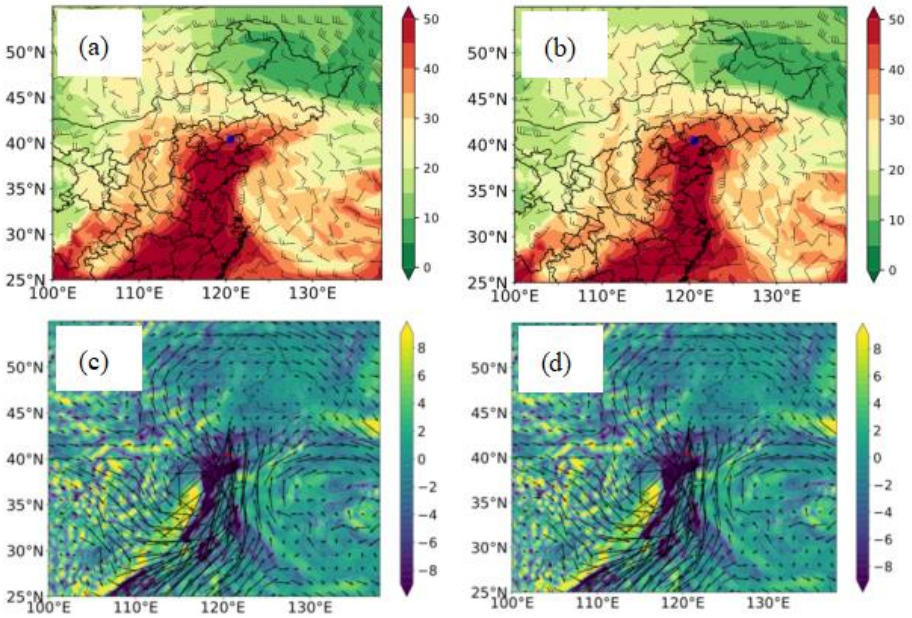

Figure 6: Atmospheric precipitable water(shaded,units:mm) with 850 hPa wind vector (arrows,units:m•s−1) at (a) 02:00 and (b) 08:00 on 20 September 2021. 1000 ~ 100 hPa vertical integral of water vapor flux (arrows,units:10 kg•m−1•s−1) and its divergence(shaded,units:10−4kg•m−2•s−1) at (c) 02:00 and 08:00 on 20 September 2021.The red and blue dots represent the location of Xingcheng.

3.5 Convective instability analysis

Convective stability is related to the vertical decreasing rate of humidity and temperature of the gas layer and the whole layer lift. The general convective stability is used to $\frac{\partial \theta_e}{\partial p}$. When $\frac{\partial \theta_e}{\partial p}$>0, the atmosphere is convectively unstable, and when $\frac{\partial \theta_e}{\partial p}$<0, the atmosphere is convectively stable. $\frac{\partial \theta_e}{\partial p}$=0 atmosphere is neutral stratification. At 20:00 on the 19th of the early precipitation period (Figure 7a), there was a warm front tilted northward at 900 hPa ~ 500 hPa, over Xingcheng, which was in front of the front, $\frac{\partial \theta_e}{\partial p}$>0, in convective instability. 950 hPa near the inverse temperature layer tilted to the south, and 850 ~ 950 hPa also had an inverse temperature tilted to the south. This may be related to the strengthening of the low-level rapids. Therefore, in the vertical direction of the lower layer is in a weak convective instability. 11:00 on the 20th (Figure7b), with the front lifting north. The maximum value of the northward lifting JAC is 346 K, while the minimum value of the cold air in the north is 312 K. The cold and warm span is large. After the front near 800 hPa there is a warm tongue, warm air masses along the front tilted up. Low-level cold air Xingcheng City is in the warm front of the low-level cold tongue, still in a weak convective instability. 20 14:00 (Figure 7c), the next hour Xingcheng City, more than 50 mm of short-term heavy precipitation. At this time Xingcheng has been in the warm front frontal isotropic dense zone. The warm and humid

atmosphere has tilted to climb to near 400 hPa, after the front is in a strong convective instability. By the time the short period of heavy precipitation weakened, because of the release of convective instability energy, Xingcheng City is in the warm front low isentropic surface dense zone. After the front from 400 hpa below the atmosphere convective instability enhanced. At 16:00 on the 20th (Figure 7d) when the precipitation process is basically over, the front and the front has been convective stability state is dominant.

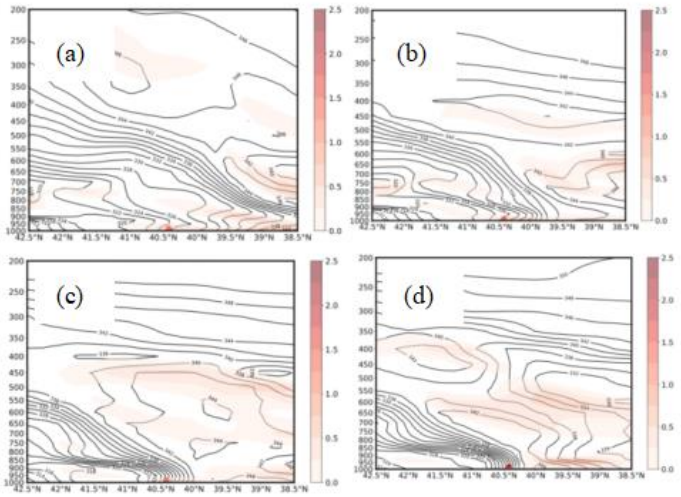

Figure 7: Meridional-vertical distribution of the equivalent potential temperature(ioline,units:K) and stratification stability $\frac{\partial \theta_e}{\partial p}$(shaded,units: 10−4 K•Pa−1) along 120.57°E at (a)08:00(b)11:00(c)14:00(d)16:00 20 on September , 2021 ,where the red dot represents the location of Xingcheng, Huludao.

3.6 Symmetric instability analysis

The wet level vortex not only characterizes the dynamic and thermal properties of the atmosphere, but also considers the role of water vapor in the atmosphere. When the wet level vortex is negative () characterizes the existence of conditional symmetric instability in the atmosphere.The wet level vortex in the P-coordinate system can be expressed as[12]:

$$MPV = -g(\zeta_p + f)\frac{\partial \theta_e}{\partial p} + g\left(\frac{\partial u}{\partial p}\frac{\partial \theta_e}{\partial y} - \frac{\partial v}{\partial p}\frac{\partial \theta_e}{\partial x}\right) MPV1 = -g(\zeta_p + f)\frac{\partial \theta_e}{\partial p}$$

$$MPV2 = g\left(\frac{\partial u}{\partial p}\frac{\partial \theta_e}{\partial y} - \frac{\partial v}{\partial p}\frac{\partial \theta_e}{\partial x}\right)$$

Where $MPV$is the wet level vortex, ζ_p is the vertical vorticity, f is the Coe-style parameter, $\theta_e$and is the equivalent level temperature. $MPV1$is the positive pressure component of the wet level vortex, which represents the role of inertial stability and convective stability. When the atmosphere is convectively unstable, $\frac{\partial \theta_e}{\partial p} > 0$, then $MPV1 < 0$. $MPV2$is the oblique pressure component of the wet level vortex, representing the wet oblique pressure term, which contains the effect of wet oblique compressibility and vertical shear of horizontal wind. The increase of the vertical shear of the wind or the increase of the horizontal wet slope pressure can cause the growth of the vertical vorticity due to the tilt of the wet isentropic surface, which is favorable to the occurrence or increase of heavy precipitation.

Figure. 8 shows the variation of the MPV、$MPV1$ and $MPV2$ with time over Xingcheng. From

20:00 on the 19th, precipitation starts to occur in the Xingcheng area, and at the beginning of the precipitation period from 20:00 on the 19th to 06:00 on the 20th, between 900 hPa and 750 hPa ~ 800 hPa, the convection over Xingcheng is $MPV1<0$, indicating the existence of convective instability in the atmosphere during this period. The profile distribution over Xingcheng in this period is similar to that of $MPV1$.The negative area between 950 hPa and 750 hPa indicates that the conditional symmetric instability may exist at low altitude. When symmetric instability and convective instability co-exist in the atmosphere, the atmosphere will be dominated by convective instability because the growth rate of convective instability is larger than that of symmetric instability[13]. Therefore, the atmosphere is dominated by convective instability during the period from 20:00 on the 19th to 06:00 on the 20th.

From 06:00 on the 20th, the lower atmosphere over Xingcheng becomes positive, indicating that the laminar stability is weakened and the lower atmosphere becomes convectively stable, while the negative areas of MPV and $MPV1<0$, there is a strong symmetric instability. There is always a negative zone in the lower layer, and cold air from the middle layer invades downward to the lower layer, and the maximum negative zone appears at 12:00 on the 20th, when precipitation is strongest. The $MPV2$ positive zone below 950 hPa gradually strengthened from 20:00 on the 19th, indicating the strengthening of warm and humid airflow and oblique pressure. At about 11:00 on the 20th, an explosive enhancement occurred, indicating that the warm and humid airflow and low-level rapids at this time suddenly strengthened. By 16:00 on the 20th, $MPV1 > 0$ below 950 hPa when the precipitation basically ended.

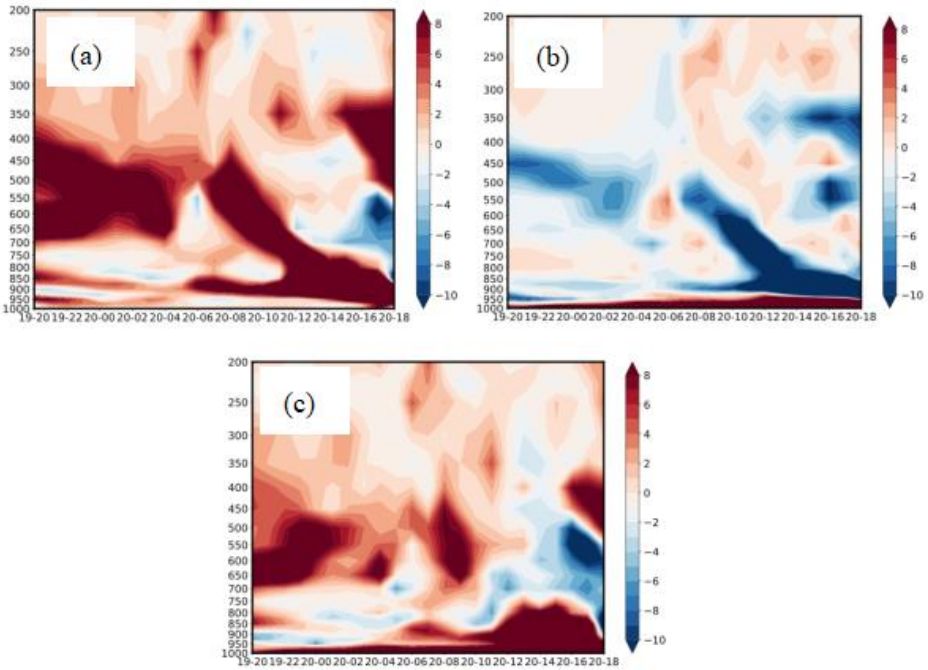

Figure 8: Height-time evolution of (a) MPV (unit: 10-1 PVU), (b) $MPV1$ (unit: 10-1 PVU) and (c) $MPV2$ (unit: 10-1 PVU), in Xingcheng(40.42 ℃N, 120.57 ℃E) from 19:00 20 September to18:00 20 September 2021

4. Conclusion

This paper presented the dynamic, thermal and water vapor characteristics of a regional extreme rainstorm in Liaoning Province on September 19, 2021 were diagnosed and analyzed, and the following preliminary conclusions were obtained.

(1) This rainstorm occurred under favorable circulation conditions. The deep trough in front of the ridge at high level provides the dynamic conditions for strong high-altitude dispersion; the mid-level high-altitude trough guides the low-level JAC cyclone northward, and the low-level and super-low-level shear lines and rapids provide water vapor and dynamic conditions. The favorable high- and low-altitude configurations caused the extreme rainstorms in Huludao and Jinzhou. Huludao has high altitude radiation dispersion and strong high altitude rapids. The low level is in the shear convergence zone of easterly and southeasterly winds at the top of a deep vortex. There are strong southeasterly rapids in the boundary layer. The cyclonic circulation is from 950 to 350 hPa over Xingcheng City, and the vertical motion extends upward to 150 hPa, and the strong rising center appears in the middle and lower layers.

(2) There are two water vapor conveyor belts for this storm, one is the low-level rapid flow through the precipitable high value area, and the other is a relatively weak water vapor conveyor belt (weaker water vapor convergence center and precipitable high value area) transported northward from the eastern part of Jiangsu through the East China Sea. The two water vapor conveyor belts converge in western Liaoning and form a water vapor flux convergence center near the Huludao and Jinzhou areas to supply water vapor for heavy rainfall. The low-level rapid flow field accompanied by the water vapor conveyor belt also has strong horizontal shear.

(3) Before the start of precipitation fronts in convective instability and symmetric instability, with the enhancement of precipitation convective instability weakened. The temperature difference between the north and south of the front is large, and there is a significant warm tongue at the lower level.Micro polypropylene fiber is more effective in reducing pore pressure than macro polypropylene fiber or steel fiber. Steel fiber plays some roles in pore pressure reduction in deeper regions, while the macro polypropylene fiber has a better effect in shallow regions than in deep regions during fire exposure. The positive hybrid effect in pore pressure reduction of steel and micro polypropylene fiber is better than that of steel fiber hybrid macro polypropylene fiber reinforced SCC. The pore pressure in SCC exposed to fire is obviously lower than that of other concrete exposed to electric heating. Larger internal destruction in SCC during fire exposure maybe explains this phenomenon.

Acknowledgements

The authors acknowledge the National Natural Science Foundation of China (Grant: 111578109), the National Natural Science Foundation of China (Grant: 11111121005).

References

[1] Tang Mingxiu, Sun Sha, Zhu Xiufang, et al. CMIP6 assessment of changes in hazard of future rainstorms in China.Advances in Earth Science, 2022, 37(5):519-534.

[2] Zhao Xianting, Min Airong, Liao Yishan, et al. Major heavy rain events in China from April to October in 2020. Torrential Rain and Disasters, 2021,40(6): 675-686.

[3] Ran Lingkun, Li Shuwen, Zhou Yushu, et al.. Observational Analysis of the Dynamic, Thermal, and Water Vapor Characteristics of the "7.20".Extreme Rainstorm Event in Henan Province, 2021. Chinese Journal of Atmospheric Sciences (in Chinese), 2021, 45(6): 1366−1383.

[4] Su Aifang, Zhang Ning, Yuan Xiaochao, et al. Comparative analysis on β-mesoscale convective systems in "7.14" extreme precipitation and "8.02" thunderstorm gale events in Henan [J]. Torrential Rain and Disasters, 2016, 35(2): 126-137.

[5] Wang Chunling, Zhang Yiping, Cui Li, et al. Analysis of environmental condition and mesoscale characteristics for a heavy rainstorm event in Spring in northeast Henan. Torrential Rain and Disasters, 2022,41(1):76-85.

[6] Su Aifang, L ü Xiaona, Cui Liman, et al. Prediction and test of optimal integrated precipitation based on similar spatial distribution of precipitation. Torrential Rain and Disasters, 2021, 40(5): 445-454.

[7] Tao Shiyan, Ding Yihui. Observational evidence of the influence of the Qinghai-Xizang (Tibet) Plateau on the

occurrence of heavy rain and severe convective storms in China. Bul1. Amer. Meteor. Soc, 62, 1982, 23-30.
[8] Gong Ying, Chen Liqiang, Sui Ming. Temporal distribution character of regional heavy rain from 2001 to 2010 in Liaoning province .Journal of Meteorology and Environment, 2011, 27(6) : 14-19.
[9] Sun Xin, Chen Chuanlei, ZhaMing et al. Diagnostic analysis of three regional rainstorms in Liaoning 2008.Journal of the Meteorological Sciences. 2010, 30(6):881-888.
[10] Liang Jun, Li Yan, Huang Ting, Et al. Comparative Analysis of Two Rainstorm Events Associated with Shear Lines in 2013 over Liaodong Peninsula. Journal of Meteorology and Environment, 2015, 33(5): 882-829.
[11] Bueh Cholaw, Zhuge Anran, Xie Zuowei, et al. Water Vapor Transportation Features and Key Synoptic-scale Systems of the "7.20" Rainstorm in Henan Province in 2021. Chinese Journal of Atmospheric Sciences (in Chinese), 2022, 46(3): 725−744.
[12] Wu Guoxiong, Cai Yaping, Tang Xiaojing. Moist potential vorticity and slantwise vorticity development [J]. Acta Meteorologica Sinica (in Chinese), 1995, 53 (4): 387–405.
[13] Bennets D A, Sharp J C. 1982. The relevance of conditional symmetric instability to the prediction of mesoscale frontal rainbands [J]. Quart. J. Roy. Meteor. Soc., 108 (457): 595–602.